Model-independent contact-interaction analysis at LC: role of electron and positron polarizations

A.A. Babich[a], P. Osland[b], A.A. Pankov[a] and N. Paver[c]

[a] Pavel Sukhoi Technical University, Gomel, 246746 Belarus

[b] Department of Physics, University of Bergen,

Allégaten 55, N-5007 Bergen, Norway

[c] Dipartimento di Fisica Teorica, Università di Trieste and

Istituto Nazionale di Fisica Nucleare, Sezione di Trieste, Trieste, Italy

1 Introduction

Generally, contact interactions (CI) represent an effective expression of a non-standard dynamics characterized by one (or more) new and very large mass scale exchanges, valid in quark and lepton reactions at the "low" energies $\sqrt{s} \ll \Lambda$ attainable by current and, perhaps, future accelerators. In this case, the new interactions and dynamical mass scales can manifest themselves only indirectly, through deviations of the measured cross sections from the Standard Model (SM) predictions that, being dimensionally suppressed by some power of $\sqrt{s}/\Lambda$, are expected to be quite small. Consequently, high energy reactions in high luminosity and high precision experiments represent a suitable tool to study such signatures. If a deviation is experimentally measured, one can try to identify the effect and the corresponding model. If, conversely, no deviation occurs within the experimental accuracy, one can assess the attainable bounds on the new coupling constants, that are essentially free parameters, by comparing theoretical deviations with experimental statistical and systematic accuracies.

Here, we refer to the fermion pair production process

$$e^+ + e^- \to f + \bar{f}, \tag{1}$$

with $f \neq t$, at an electron-positron Linear Collider (LC) with c.m. energy $\sqrt{s} = 0.5\,\mathrm{TeV}$ and polarized electron and positron beams, and to the general, $SU(3) \times SU(2) \times U(1)$ symmetric $eeff$ dimension $D = 6$ contact-interaction Lagrangian, with helicity-conserving and flavor-diagonal fermion currents [1]:

$$\mathcal{L}_{\mathrm{CI}} = \frac{1}{1+\delta_{ef}} \sum_{i,j} g^2_{\mathrm{eff}}\, \epsilon_{ij} \left(\bar{e}_i \gamma_\mu e_i\right) \left(\bar{f}_j \gamma^\mu f_j\right). \tag{2}$$

In Eq. (2): $i, j = \mathrm{L}, \mathrm{R}$ denote left- or right-handed helicities, generation and color indices have been suppressed, and the CI coupling constants are parameterized in terms of corresponding mass scales as $\epsilon_{ij} = \eta_{ij}/\Lambda^2_{ij}$ with $\eta_{ij} = \pm 1, 0$ depending on the chiral structure of the individual interactions. Also, conventionally $g^2_{\mathrm{eff}} = 4\pi$, as a reminder that, in the case of compositeness, the new interaction would become strong at $\sqrt{s}$ of the order of Λ_{ij}. Obviously, deviations from the SM and upper bounds or exclusion ranges for the CI couplings can be equivalently expressed as lower bounds and exclusion ranges for the corresponding mass scales Λ_{ij}.

For a given final fermion flavor, apart from the $\pm$ signs, Eq. (2) envisages four individual, and independent, CI couplings in the case $f \neq e$ and three couplings in the elastic $f = e$ case. Correspondingly, the most general (and model-independent) analysis of the process (1) must account for the complicated situation where the full Eq. (2) is included in the expression for the cross section, and all CI couplings can appear there simultaneously as free, non-vanishing, parameters. Although by themselves the helicity amplitudes do not interfere, the numerical constraints on CI couplings can be considerably weakened due to potential cancellations of deviations of helicity amplitudes with opposite signs.

A simplifying procedure is to assume non-zero values for only one of the couplings (or one specific combination of them) at a time with all others set to zero, which would avoid problems associated with negative interference, and leads to tests of *specific* CI models only.

On the other hand, it should be highly desirable to apply a more general kind of experimental data analysis that simultaneously includes all terms of Eq. (2) as independent free parameters and, at the same time, allows the derivation of separate constraints (or exclusion regions) on the individual coupling constants. A strong possibility in this regard is offered by the availability of initial electron and positron longitudinal beam polarizations, that enable to extract from the measured data the individual helicity cross sections σ_{ij} through the definition of particular, and optimal, polarized integrated cross sections and, consequently, to disentangle the constraints on the corresponding CI coupling constants ϵ_{ij} [2, 3, 4]. Accordingly, a model-independent approach, in the sense stated above, is obtained. Also, it is a well-known fact that, when both the electron and positron beams are polarized, the total annihilation cross section into fermion-antifermion pairs will be increased by a factor [5, 6] and, in principle, one could expect a corresponding increase in sensitivity to the new parameters.

2 Polarized observables for contact interactions

The analysis of contact-interactions of Ref. [2], that we are briefly summarizing here, is limited to the cases $f \neq e, t$ where the SM is determined by only s-channel γ and Z exchanges and external fermion masses are negligible, and uses as basic observables, to be determined from angular integration of differential rates of events observed with longitudinally polarized beams, the (unpolarized) total cross section $\sigma_{\rm unpol}$ and forward-backward asymmetry $A_{\rm FB}$, the left-right asymmetry $A_{\rm LR}$ and left-right forward-backward asymmetry $A_{\rm LR,FB}$. These are defined, in the notation of Ref. [7], as:

$$\sigma_{\rm unpol} = \frac{1}{4}\left[\sigma_{\rm LL} + \sigma_{\rm LR} + \sigma_{\rm RR} + \sigma_{\rm RL}\right], \tag{3}$$

$$A_{\rm FB} = \frac{3}{4}\,\frac{\sigma_{\rm LL} - \sigma_{\rm LR} + \sigma_{\rm RR} - \sigma_{\rm RL}}{\sigma_{\rm LL} + \sigma_{\rm LR} + \sigma_{\rm RR} + \sigma_{\rm RL}}, \tag{4}$$

$$A_{\rm LR} = \frac{\sigma_{\rm LL} + \sigma_{\rm LR} - \sigma_{\rm RR} - \sigma_{\rm RL}}{\sigma_{\rm LL} + \sigma_{\rm LR} + \sigma_{\rm RR} + \sigma_{\rm RL}}, \tag{5}$$

and

$$A_{\rm LR,FB} = \frac{3}{4}\,\frac{\sigma_{\rm LL} - \sigma_{\rm RR} + \sigma_{\rm RL} - \sigma_{\rm LR}}{\sigma_{\rm LL} + \sigma_{\rm RR} + \sigma_{\rm RL} + \sigma_{\rm LR}}. \tag{6}$$

The deviations of these observables from the SM predictions are easily expressed in terms of SM couplings and the CI ones, ϵ_{ij}, of Eq. (2).

The reach at the LC on the CI couplings, and the corresponding constraints on their allowed values in the case of no indirect effect observed, can be estimated by comparing the expression of the theoretical deviations determined by the ϵ_{ij} with the foreseen experimental (statistical and systematic) uncertainties. The correlation among uncertainties on the four basic observables can be taken into account *via* the method of the covariance matrix [8, 9].

As numerical inputs, we assume as reference values the identification efficiencies [10]: 95%, 60% and 35% for the channels for l^+l^-, $b\bar{b}$ and $c\bar{c}$, respectively. To assess the relative roles of statistical and systematic uncertainties, we vary the time-integrated luminosity $\mathcal{L}_{\rm int}$ from 50 to 500 fb^{-1} with uncertainty $\delta\mathcal{L}_{\rm int}/\mathcal{L}_{\rm int} = 0.5\%$, and a fiducial experimental angular range $|\cos\theta| \leq 0.99$. Regarding electron and positron degrees of polarization, we consider the values: $|P_e| = 0.8$; $|P_{\bar{e}}| = 0.0$, and 0.6, with the uncertainties $\delta P_e/P_e = \delta P_{\bar{e}}/P_{\bar{e}} = 0.5$ %.

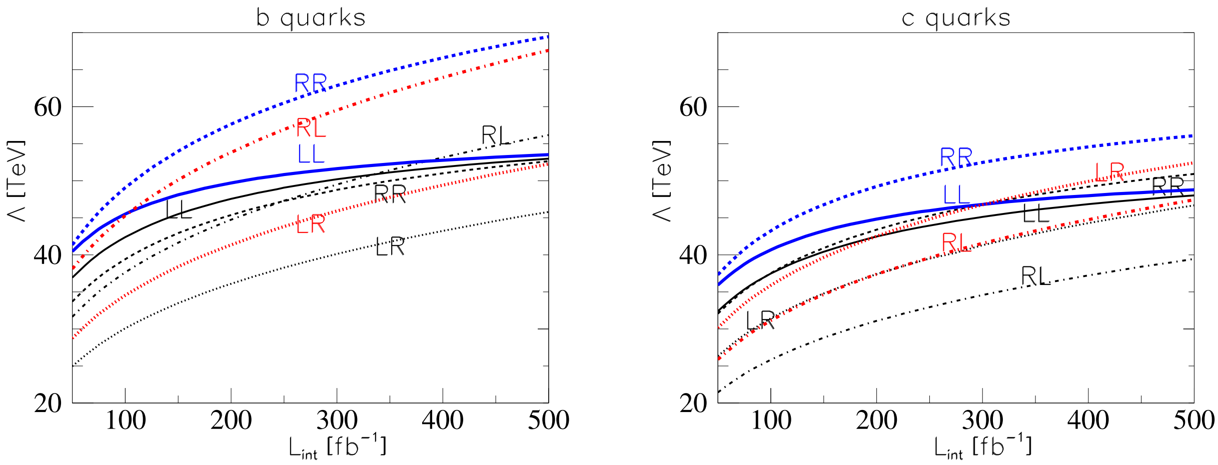

Figure 1: Contact-interaction scale Λ vs. integrated luminosity, $\mathcal{L}_{\rm int}$, for b and c quarks, and for the four helicity combinations. Thin curves: $P_e = 0.8$, $P_{\bar{e}} = 0$, heavy curves: $P_e = 0.8$, $P_{\bar{e}} = 0.6$.

The model-independent bounds on the mass scales Λ_{ij} at the 95% C.L. allowed by the experimental uncertainties reported above are shown in Figs. 1 and 2 for the considered annihilation channels, respectively. In these figures, heavy curves correspond to $|P_e| = 0.8, |P_{\bar{e}}| = 0.6$ while thin curves correspond to $|P_e| = 0.8, |P_{\bar{e}}| = 0.0$.

As one can see from Eqs. (3) and (4), without simplifying assumptions in the unpolar-

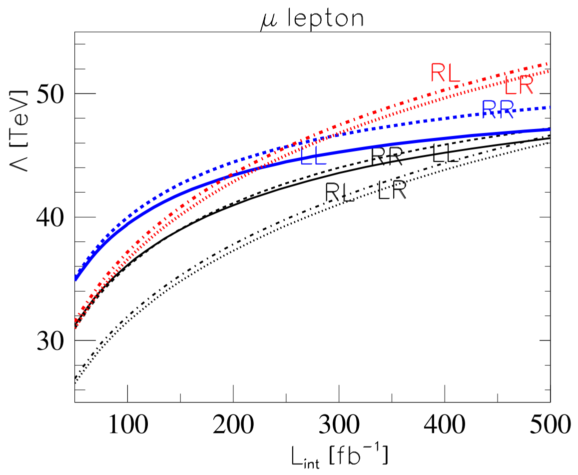

Figure 2: Same as Fig. 1, for muons. (Note other scale.)

ized case the CI couplings could not be individually constrained within finite ranges, but only mutual correlations could be derived. With initial longitudinal beam polarization, the two additional available physical observables (5) and (6) are essential to obtain finite, model-independent, bounds. In principle, electron beam polarization would be sufficient to achieve this result but, depending on the luminosity and the final $f\bar{f}$ channel, a significant increase on the sensitivity to CI couplings can arise from the additional availability of positron polarization.

3 CI analysis in Bhabha and Møller scattering

With $\delta_{ef} = 1$ the four-fermion contact interaction Lagrangian of Eq. (2) is relevant to the Bhabha scattering process

$$e^+ + e^- \rightarrow e^+ + e^-, \tag{7}$$

as well as to Møller scattering:

$$e^- + e^- \rightarrow e^- + e^-. \tag{8}$$

The possibility of studying new physics in the process (8) at the LC by turning the positron beam into an electron beam has been considered with interest and, therefore, it should be useful to assess (and compare) the sensitivities of the two processes to the four-electron CI constants of Eq. (2) by a model-independent analysis that simultaneously accounts for all ϵ's as free parameters.

Different from the annihilation processes considered in Sect. 2, in the case of processes (7) and (8), apart from the $\pm$ signs, there are only three (not four) independent CI couplings: $\epsilon_{\rm LL}$, $\epsilon_{\rm RR}$ and $\epsilon_{\rm LR} = \epsilon_{\rm RL}$ (same ϵ's for the two processes). The other principal difference, that complicates the procedure to disentangle the constraints on individual couplings, is that Bhabha scattering is determined, in the SM, by γ and Z exchanges in both the s- and t-channels, while Møller scattering is determined by γ and Z poles in both the t- and u-channels.

3.1 Bhabha scattering

With *both* electron and positron beams longitudinally polarized, one can assume that the polarization of each beam can be changed on a pulse by pulse basis, which would allow the separate measurements of the polarized differential cross sections $\mathrm{d}\sigma_{++}$, $\mathrm{d}\sigma_{+-}$ and $\mathrm{d}\sigma_{-+}$, corresponding to the configurations of beam polarizations $(P_e, P_{\bar{e}}) = (P_1, P_2)$, $(P_1, -P_2)$ and $(-P_1, P_2)$, respectively, with $P_{1,2} > 0$ [11]. They are related to combinations of helicity cross sections $\mathrm{d}\sigma_{\rm R}$, $\mathrm{d}\sigma_{\rm L}$ and $\mathrm{d}\sigma_{{\rm LR},t}$ containing the CI couplings and therefore representing the basic observables for the analysis, by a system of linear equations of the form [11]:

$$\begin{aligned}
\mathrm{d}\sigma_{\rm R} &= \frac{(1+P_2)^2}{2P_2(P_1+P_2)}\,\mathrm{d}\sigma_{+-} + \frac{(1-P_1)^2}{2P_1(P_1+P_2)}\,\mathrm{d}\sigma_{-+} - \frac{1-P_1P_2}{2P_1P_2}\,\mathrm{d}\sigma_{++},\\
\mathrm{d}\sigma_{\rm L} &= \frac{(1-P_2)^2}{2P_2(P_1+P_2)}\,\mathrm{d}\sigma_{+-} + \frac{(1+P_1)^2}{2P_1(P_1+P_2)}\,\mathrm{d}\sigma_{-+} - \frac{1-P_1P_2}{2P_1P_2}\,\mathrm{d}\sigma_{++},\\
\mathrm{d}\sigma_{{\rm LR},t} &= -\frac{1-P_2^2}{2P_2(P_1+P_2)}\,\mathrm{d}\sigma_{+-} - \frac{1-P_1^2}{2P_1(P_1+P_2)}\,\mathrm{d}\sigma_{-+} + \frac{1+P_1P_2}{2P_1P_2}\,\mathrm{d}\sigma_{++}.
\end{aligned} \tag{9}$$

It turns out that, while $\sigma_{{\rm LR},t}$ (that is pure t-pole) depends on a single contact interaction parameter ($\epsilon_{\rm LR}$), which therefore can be *directly* disentangled from the other couplings, $\sigma_{\rm R}$ and $\sigma_{\rm L}$ simultaneously depend on *pairs* of parameters, ($\epsilon_{\rm RR}$,$\epsilon_{\rm LR}$) and ($\epsilon_{\rm RR}$,$\epsilon_{\rm LR}$), respectively, and in this case (ellipsoidal) allowed areas in the relevant planes can be obtained. This clearly shows that *both* electron *and* positron polarization are needed to perform a model-independent analysis of CI couplings in Bhabha scattering. One can easily see that, without polarization ($P_1 = P_2 = 0$), in the general case only correlations among couplings can be derived and, in particular, the contribution of $\epsilon_{\rm LR}$ is subject to partial cancellations.

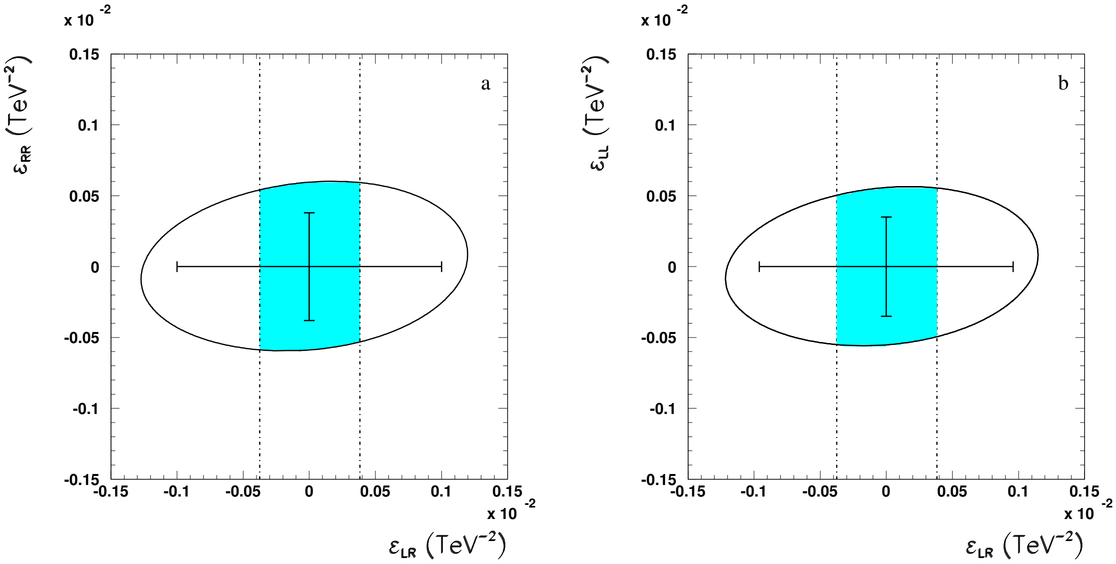

Figure 3: Allowed areas at 95% C.L. in the planes $(\epsilon_{\rm LR}, \epsilon_{\rm RR})$ and $(\epsilon_{\rm LR}, \epsilon_{\rm LL})$ obtained from $\sigma_{\rm R}$ and $\sigma_{\rm L}$ in $e^+e^- \to e^+e^-$ at $\sqrt{s} = 0.5$ TeV, $\mathcal{L}_{\rm int}(e^+e^-) = 50$ fb^{-1}, $|P_e| = 0.8$, $|P_{\bar{e}}| = 0.6$. Vertical dashed lines indicate the range allowed to $\epsilon_{\rm LR}$ by $\sigma_{{\rm LR},t}$.

To assess the sensitivity of Bhabha scattering to the compositeness scale, in Fig. 3 we depict as an example the 95% C.L. contours around $\epsilon_{\rm LL} = \epsilon_{\rm RR} = \epsilon_{\rm LR}$ in the two-dimensional planes ($\epsilon_{\rm RR}$,$\epsilon_{\rm LR}$) and ($\epsilon_{\rm RR}$,$\epsilon_{\rm LR}$), derived from a χ^2 analysis of differential cross sections, assuming that no deviation from the SM within the experimental uncertainty (statistical and systematic) is measured in d$\sigma_{\rm L}$, d$\sigma_{\rm R}$ and d$\sigma_{{\rm LR},t}$ ($\mathcal{L}_{\rm int}(e^+e^-) = 50$ fb^{-1}, $P_1 = 0.8$, $P_2 = 0.6$, $\delta\mathcal{L}_{\rm int}/\mathcal{L}_{\rm int} = \delta P_1/P_1 = \delta P_2/P_2 = 0.5\%$). The crosses indicate the constraints obtained by taking one non-zero parameter at a time instead of two simultaneously non-zero and independent.

In Fig. 4 we show the maximum reachable values (95% C.L.) on the mass scales Λ as a funtion of the time-integrated luminosity at the LC. The dramatic sensitivity of process (7) to $\Lambda_{\rm LR}$, that can be disentangled directly owing to polarization, is clearly shown by this figure.

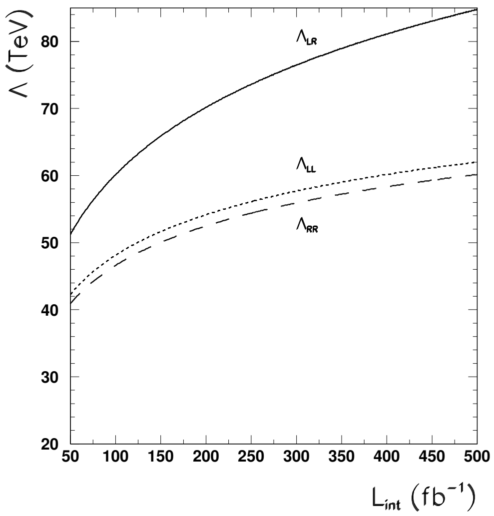

Figure 4: Model-independent reach on Λ at 95% C.L. vs. $\mathcal{L}_{\rm int}(e^+e^-)$ from $e^+e^- \to e^+e^-$ at $\sqrt{s} = 0.5$ TeV, $|P_e| = 0.8$, $|P_{\bar{e}}| = 0.6$.

3.2 Møller scattering with polarized electrons

Similar to process (7), in this case the SM amplitudes have both t- and u-poles. However, there is an outstanding difference: denoting by $P_e^{(1)}$ and $P_e^{(2)}$ the degree of initial electron longitudinal polarization, and by $\mathrm{d}\sigma_{++}$, $\mathrm{d}\sigma_{--}$ and $\mathrm{d}\sigma_{+-}$ the measurable polarized differential cross sections corresponding to the three configurations $(P_e^{(1)}, P_e^{(2)}) = (P_1, P_2)$, $(-P_1, -P_2)$ and $(P_1, -P_2)$, respectively, with $P_{1,2} > 0$, the analogue of the system of linear equations (9) is [11]:

$$\begin{aligned}
\mathrm{d}\sigma_{\rm RR} &= \frac{(1+P_2)^2}{2P_2(P_1+P_2)}\,\mathrm{d}\sigma_{++} + \frac{(1-P_1)^2}{2P_1(P_1+P_2)}\,\mathrm{d}\sigma_{--} - \frac{1-P_1P_2}{2P_1P_2}\,\mathrm{d}\sigma_{+-}, \\
\mathrm{d}\sigma_{\rm LL} &= \frac{(1-P_2)^2}{2P_2(P_1+P_2)}\,\mathrm{d}\sigma_{++} + \frac{(1+P_1)^2}{2P_1(P_1+P_2)}\,\mathrm{d}\sigma_{--} - \frac{1-P_1P_2}{2P_1P_2}\,\mathrm{d}\sigma_{+-}, \\
\mathrm{d}\sigma_{\rm LR} &= -\frac{1-P_2^2}{2P_2(P_1+P_2)}\,\mathrm{d}\sigma_{++} - \frac{1-P_1^2}{2P_1(P_1+P_2)}\,\mathrm{d}\sigma_{--} + \frac{1+P_1P_2}{2P_1P_2}\,\mathrm{d}\sigma_{+-},
\end{aligned} \tag{10}$$

and each of the cross sections $\sigma_{\rm RR}$, $\sigma_{\rm LL}$ *and* $\sigma_{\rm LR}$ depend on an individual contact-interaction parameter. Therefore, complete disentangling of the various CI couplings (hence the derivation of model-independent constraints) is *directly* achieved in the Møller process with both beams polarized.

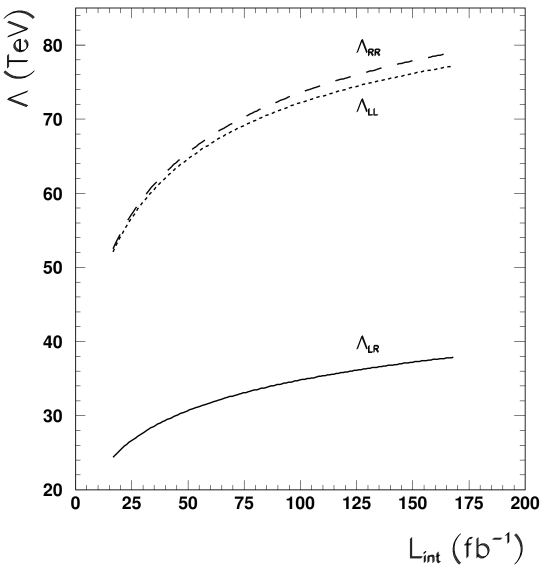

Figure 5: Model-independent reach on Λ at 95% C.L. vs. $\mathcal{L}_{\rm int}(e^-e^-)$ from $e^-e^- \to e^-e^-$ at $\sqrt{s} = 0.5$ TeV and $|P_e^{(1)}| = |P_e^{(2)}| = 0.8$.

In Fig. 5 we report the 95% C.L. model-independent reach on Λ's vs. the integrated luminosity, that can be attained from process (8) at the LC with $\sqrt{s} = 0.5$ TeV and both initial electrons longitudinally polarized with $P_1 = P_2 = 0.8$ (systematic uncertainties are assumed to be the same as in the previous case). As regards the range of values of the luminosity, we have taken into account that $\mathcal{L}_{\rm int}(e^-e^-)$ at the linear collider is expected to be somewhat reduced by anti-pinching compared to $\mathcal{L}_{\rm int}(e^+e^-)$, typically by a factor 1/7 to 1/3, which, of course, tends to depress the sensitivity to the new physics. One can see, compared to Fig. 4, the higher sensitivity of the polarized process (8) to $\Lambda_{\rm LL}$ and $\Lambda_{\rm RR}$ with respect to $\Lambda_{\rm LR}$.

One can conclude, finally, as far as the sensitivity to individual couplings in a model-independent data analysis is concerned that, if $\mathcal{L}_{\rm int}(e^-e^-)$ is not too low, the two processes (7) and (8) are somehow complementary. Also, the advantage of having both initial beams polarized, that allows the measurement of suitable polarized cross sections in order to disentangle the different contact-interaction couplings, is clear.

4 Identification of graviton exchange effects

Process (1) at the LC has been considered with much interest as a tool to look for effects related to large extra dimensions and low-scale gravity [12, 13], in particular the virtual effects from KK graviton exchange. This effect can in the ADD scenario [12] be modeled, in the framework of contact interactions, by the effective Lagrangian [14]

$$\mathcal{L} = i\frac{4\lambda}{M_H^4}T_{\mu\nu}T^{\mu\nu}, \tag{11}$$

where $T_{\mu\nu}$ is the energy-momentum tensor, M_H is the relevant graviton cut-off mass scale and λ is a sign factor ($\lambda = \pm 1$). In principle, one could apply the same arguments as outlined in the previous sections to derive the sensitivity to (11) and the corresponding reach on M_H by considering the deviations from the Standard Model predictions caused by this kind of interaction and numerically comparing them to the foreseen experimental uncertainties on the cross sections. Actually, since there is only one coupling, polarization would not be strictly required, and the only difference that remains would be that, compared to the previous contact-interaction Lagrangian (2), being induced by a dimension $D = 8$ operator the KK graviton exchange is suppressed by the much higher power $(\sqrt{s}/M_H)^4$, so that a lower reach on M_H can be expected in comparison to the constraints obtainable, at the same c.m. energy, on the Λ's.

On the other hand, due to its spin-2 character, the deviations produced by KK exchange in the helicity amplitudes of process (1) have a specific angular dependence, whereas those from the interactions represented by (2), due to their vector current-current form, have a different angular dependence. Accordingly, for final $f\bar{f}$ channels with $f \neq e$ dominated in the SM by s-channel γ and Z exchanges, there is the possibility of uniquely identifying in the data analysis the effects of graviton exchange from other new physics.

In this connection, a particularly suitable observable is represented by the generalized centre-edge asymmetry among integrated differential distributions [15]:

$$A_{\rm CE} = \frac{\sigma_{\rm CE}}{\sigma}, \tag{12}$$

with

$$\sigma_{\rm CE} = \left[\int_{-z^*}^{z^*} - \left(\int_{-1}^{-z^*} + \int_{z^*}^{1}\right)\right]\frac{\mathrm{d}\sigma}{\mathrm{d}z}\,\mathrm{d}z, \qquad \sigma = \int_{-1}^{1}\frac{\mathrm{d}\sigma}{\mathrm{d}z}\,\mathrm{d}z \tag{13}$$

and $0 < z^* < 1$ (here, $z = \cos\theta$ with θ the angle between electron and outgoing fermion in the c.m.).

A crucial feature of $A_{\rm CE}$ is that it is *identical* to that of the SM even if contact-interaction-like interactions are present:

$$A_{\rm CE}^{\rm SM+CI} \equiv A_{\rm CE}^{\rm SM+CI} = \frac{1}{2}z^*\left(z^{*2}+3\right) - 1, \tag{14}$$

independent of final-state flavour, energy, and longitudinal beam polarization and therefore, for these interactions, there is no deviation. Conversely, $A_{\rm CE}$ with graviton exchange is *different* and *does* depend on final state flavor and initial beam polarization, and the largest deviation $\Delta A_{\rm CE}$ from $A_{\rm CE}^{\rm SM}$ is produced by the interference of the SM with Eq. (11). Therefore, the asymmetry (12) has the property of "filtering out" the "conventional" contact interactions represented by the Lagrangian (2) from deviations from the SM, and consequently of providing a clear signature for graviton exchange, particularly for choices of z^* around the value $z_0^* = 0.596$ where the right-hand side of (14) vanishes and the effect (hence, the sensitivity) is maximal.

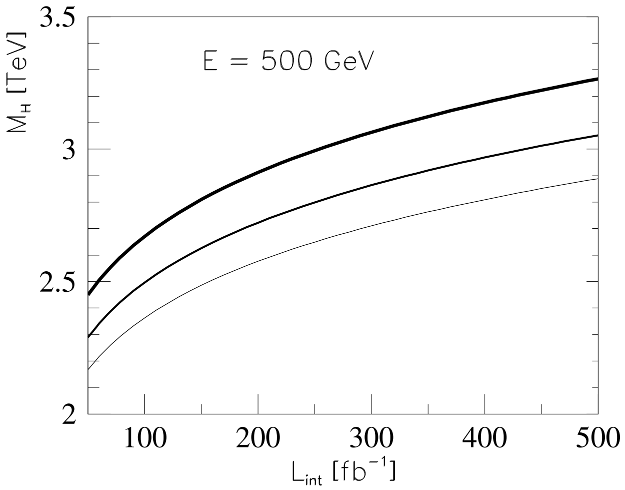

Figure 6: 5σ reach on the mass scale M_H *vs.* integrated luminosity from the process $e^+e^- \to f\bar{f}$, with f summed over μ, τ, b, c, and for the energy 0.5 TeV. Thin: unpolarized; medium: electrons polarized, $P_e = 0.8$; heavy: both beams polarized, $P_e = 0.8$, $P_{\bar{e}} = -0.6$.

In Fig. 6 we present, as an example, the 5σ identification reach on the mass scale M_H, summing over the channels $f = \mu, \tau, b, c$, that can be obtained at the LC by a χ^2

analysis assuming that no deviation $\Delta A_{\rm CE}$ is seen within the experimental accuracy, with the same assumptions on the integrated luminosity and the initial beam polarization (and the corresponding uncertainties) considered previously. Thin, medium and heavy curves refer, respectively, to the cases $(P_e = P_{\bar{e}} = 0)$, $(P_e = 0.8, P_{\bar{e}} = 0)$ and $(P_e = 0.8, P_{\bar{e}} = 0.6)$.

Longitudinal beam polarization appears to increase the sensitivity to graviton exchange, although the impact on M_H is less dramatic in this case due to the suppression $(\sqrt{s}/M_H)^4$ of the graviton coupling. Instead, initial polarization can be seen to play a key role in distinguishing graviton exchange from competing effects, such as those originating from scalar particle exchange in both s- and t-channels, that can be "filtered" out by appropriate polarization asymmetries [15, 16].

References

[1] E. Eichten, K. Lane and M. E. Peskin, Phys. Rev. Lett. **50** (1983) 811;
R. Rückl, Phys. Lett. B **129** (1983) 363.

[2] A. A. Babich, P. Osland, A. A. Pankov and N. Paver, Phys. Lett. B **518** (2001) 128 [hep-ph/0107159].

[3] A. A. Babich, P. Osland, A. A. Pankov and N. Paver, LC Note LC-TH-2001-021 (2001), hep-ph/0101150.

[4] A. A. Babich, P. Osland, A. A. Pankov and N. Paver, Phys. Lett. B **481** (2000) 263 [hep-ph/0003253].

[5] K. Flottmann, DESY-95-064;

[6] K. Fujii and T. Omori, KEK-PREPRINT-95-127.

[7] B. Schrempp, F. Schrempp, N. Wermes and D. Zeppenfeld, Nucl. Phys. B **296** (1988) 1.

[8] W.T. Eadie, D. Drijard, F.E. James, M. Roos, B. Sadoulet, *Statistical methods in experimental physics* (American Elsevier, 1971).

[9] F. Cuypers and P. Gambino, Phys. Lett. B **388** (1996) 211 [hep-ph/9606391]; F. Cuypers, hep-ph/9611336.

[10] C. J. S. Damerell, D.J. Jackson, in *Proceedings of the 1996 DPF/DPB Summer Study on New Directions for High Energy Physics* (Snowmass 96), Edited by D.G. Cassel, L. Trindle Gennari, R.H. Siemann (SLAC, 1997) p. 442.

[11] A. A. Pankov and N. Paver, [hep-ph/0209058], to appear in Eur. Phys. J. C.

[12] N. Arkani-Hamed, S. Dimopoulos and G. R. Dvali, Phys. Lett. B **429** (1998) 263 [hep-ph/9803315].

[13] For a review see, *e.g.*, J. Hewett and M. Spiropulu, Ann. Rev. Nucl. Part. Sci. **52** (2002) 397 [hep-ph/0205106].

[14] J. L. Hewett, Phys. Rev. Lett. **82** (1999) 4765 [hep-ph/9811356].

[15] P. Osland, A. A. Pankov and N. Paver, [hep-ph/0304123], to be published in Phys. Rev. D.

[16] T. G. Rizzo, Phys. Rev. D **59** (1999) 113004 [hep-ph/9811440].